

POWER FLOW IN A MULTI-TERAWATT RADIATION SOURCE*

E. Nolting, L. Miles, J. Miller, J. Draper, V. Kenyon, III^a, W. Spicer, Jr.^b, C. Parsons, and
F. Warnock
Carderock Division, Naval Surface Warfare Center, White Oak Laboratory,
Silver Spring, MD 20903-5640

A. Fisher, G. Peterson^c, and R. Terry
Naval Research Laboratory, Washington, D.C. 20375-5346

M. Krishnan^d, R. Prasad^d, and G. Rondeau^e
Science Research Laboratory, Inc. Sommerville, MA 02143

J. Fockler, P. Spence, I. Smith, and P. Corcoran
Titan Pulse Sciences Incorporated, San Leandro, CA 94577

R. Smith
Advanced Technology and Research, Burtonsville, MD 20866-1172

Abstract

Much of the research emphasis in the development of z-pinches as intense x-ray sources has been directed toward increasing the power flow into the load. Near the load, linear current densities in excess of 500 kA/cm are not uncommon. To achieve these very high power flow density levels, it is necessary to construct low-inductance (a few nanohenries), sub-ohm impedance, vacuum transmission lines. These transmission lines depend upon the current's self-magnetic fields to prevent significant electron flow across the millimeter gaps separating the highly stressed electrodes. Because of the intense radiation generated by the plasma source and its time varying nature, power flow from the source can be diverted from the load and reduce the radiation output. This limitation in the power delivered to the plasma is recognized as a major impediment to increasing radiation output. A variety of geometrical and radiation environment considerations make it difficult to develop monitors which can accurately determine the current loss by direct measurement. In general, the difficulty in making these critical measurements increases as the linear current density increases near the source. This paper describes some of the techniques used on the Phoenix radiation effects simulator to measure and improve its output, along with results from these efforts. In particular, a discussion of vacuum power flow including the main features of a new insulator stack design will be presented, along with a description of some of the unique features of the Phoenix gas valve design, the results of simulator prepulse measurements, and the implication of prepulse on simulator performance.

I: Introduction

When operated as a plasma radiation source (PRS), the Phoenix simulator uses standard pulse power technology to deliver a nominal five terawatt power pulse to the load, see Figure 1. The Phoenix marx is comprised of three parallel marx banks. The total erected capacity of the three-34 stage marx banks is 93 nF, with an effective inductance of approximately 7 μ H, and a total internal resistance of about 1 Ω . Each stage is comprised of two, series-connected 2.1 μ F, 100 kV capacitors. When charged to its maximum voltage (± 87 kV per stage), the total energy stored in the marx is 1.6 MJ and has an open circuit voltage of 5.9 MV. The marx charges the 62 nF transfer capacitor in approximately 1.3 μ sec.

The transfer capacitor is used to charge a 50 ns long, 1.3 Ω (39 nF), coaxial, pulse

Report Documentation Page		Form Approved OMB No. 0704-0188
Public reporting burden for the collection of information is estimated to average 1 hour per response, including the time for reviewing instructions, searching existing data sources, gathering and maintaining the data needed, and completing and reviewing the collection of information. Send comments regarding this burden estimate or any other aspect of this collection of information, including suggestions for reducing this burden, to Washington Headquarters Services, Directorate for Information Operations and Reports, 1215 Jefferson Davis Highway, Suite 1204, Arlington VA 22202-4302. Respondents should be aware that notwithstanding any other provision of law, no person shall be subject to a penalty for failing to comply with a collection of information if it does not display a currently valid OMB control number.		
1. REPORT DATE JUL 1995	2. REPORT TYPE N/A	3. DATES COVERED -
4. TITLE AND SUBTITLE Power Flow In A Multi-Terawatt Radiation Source		5a. CONTRACT NUMBER
		5b. GRANT NUMBER
		5c. PROGRAM ELEMENT NUMBER
6. AUTHOR(S)	5d. PROJECT NUMBER	
	5e. TASK NUMBER	
	5f. WORK UNIT NUMBER	
7. PERFORMING ORGANIZATION NAME(S) AND ADDRESS(ES) Carderock Division, Naval Surface Warfare Center, White Oak Laboratory, Silver Spring , MD 20903-5640		8. PERFORMING ORGANIZATION REPORT NUMBER
9. SPONSORING/MONITORING AGENCY NAME(S) AND ADDRESS(ES)		10. SPONSOR/MONITOR'S ACRONYM(S)
		11. SPONSOR/MONITOR'S REPORT NUMBER(S)
12. DISTRIBUTION/AVAILABILITY STATEMENT Approved for public release, distribution unlimited		
13. SUPPLEMENTARY NOTES See also ADM002371. 2013 IEEE Pulsed Power Conference, Digest of Technical Papers 1976-2013, and Abstracts of the 2013 IEEE International Conference on Plasma Science. Held in San Francisco, CA on 16-21 June 2013. U.S. Government or Federal Purpose Rights License.		
14. ABSTRACT Much of the research emphasis in the development of z-pinches as intense x-ray sources has been directed toward increasing the power flow into the load. Near the load, linear current densities in excess of 500 kNcm are not uncommon. To achieve these very high power flow density levels, it is necessary to construct low-inductance (a few nanohenries), sub-ohm impedance, vacuum transmission lines. These transmission lines depend upon the current's selfmagnetic fields to prevent significant electron flow across the millimeter gaps separating the highly stressed electrodes. Because of the intense radiation generated by the plasma source and its time varying nature, power flow from the source can be diverted from the load and reduce the radiation output. This limitation in the power delivered to the plasma is recognized as a major impediment to increasing radiation output. A variety of geometrical and radiation environment considerations make it difficult to develop monitors which can accurately determine the current loss by direct measurement. In general, the difficulty in making these critical measurements increases as the linear current density increases near the source. This paper describes some of the techniques used on the Phoenix radiation effects simulator to measure and improve its output, along with results from these efforts. In particular, a discussion of vacuum power flow including the main features of a new insulator stack design will be presented, along with a description of some of the unique features of the Phoenix gas valve design, the results of simulator prepulse measurements, and the implication of prepulse on simulator performance.		
15. SUBJECT TERMS		

16. SECURITY CLASSIFICATION OF:			17. LIMITATION OF ABSTRACT SAR	18. NUMBER OF PAGES 7	19a. NAME OF RESPONSIBLE PERSON
a. REPORT unclassified	b. ABSTRACT unclassified	c. THIS PAGE unclassified			

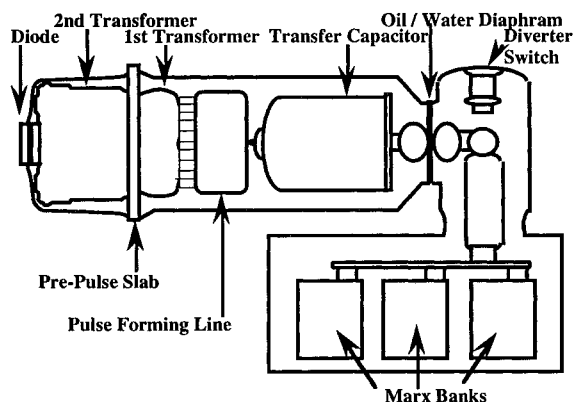


Figure 1 Basic Phoenix pulse power circuit

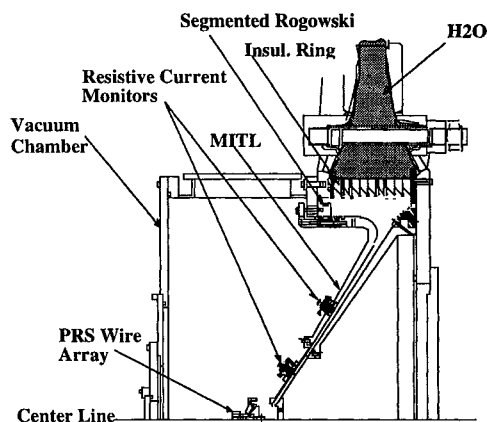


Figure 2. Schematic of Phoenix PRS diode with new insulator design.

forming line (PFL) through a single channel, self-closing, water-dielectric switch. The PFL is switched out through a set of 30, over-volted, water-dielectric switches into a 1.2Ω transmission line. This transmission line is broken by a 35.7 cm (14") thick epoxy slab containing 20 self-actuated gas switches which are used to reduce the diode prepulse voltage. Energy flow from the prepulse switches is into a 1.5Ω line that is smoothly tapered to $3/8 \Omega$ at the entrance to the diode. Figure 2 illustrates the basic diode geometry. Inside the vacuum envelope, power is delivered by a magnetically insulated transmission line (MITL) that is formed of two distinct sections. A constant impedance section, which places the MITL electrodes at fixed angular separation, and a constant gap section, which causes the impedance to increase toward the load. MITL adjustment is made by setting the spacing in the constant gap section. Although this configuration produces a low inductance diode, one concern with this geometry is the relatively straight line-of-sight path from the plasma source to the insulator stack. This presents the possibility of premature insulator flashover due to ultraviolet illumination of the insulators.

The diode has been used to drive both imploding wire assemblies and gas puff discharges. A typical wire array is formed by 16-0.8 mil (20 μm) diameter aluminum wires evenly spaced on a 2.5 cm diameter circle, the length of the wire array is 4 cm; wire holders have been made of both tellurium-copper and stainless steel. A return current cage arrangement with eight evenly spaced, 0.24 cm diameter, stainless steel rods on a 5 cm diameter circle is used to complete the electrical circuit. The geometry of the gas valve is shown in Figure 3. The gas valve is designed to give a relatively fast rise pressure pulse and reaches steady-state-flow conditions in about 250 μsec . This has been achieved by minimizing the flow path from the valve to the nozzle, and providing a high conductance connection to the nozzle throat. Measurements, based on upon hundreds of shots, have shown the output to be very repeatable ¹. A typical gas puff configuration has a 3.5 cm mean nozzle diameter with a 13.75° inward tilt (toward the axis of symmetry), and a 4 cm separation between the anode and cathode. The nozzle has a 5 mil (125 μm) annular throat spacing that produces on the order of Mach 3 flow velocities. The return current cage is made of eight, uniformly-spaced, stainless steel bars (12.7 mm radial direction by 2.4 mm azimuthal direction) that provide a clear view of the PRS. The length of the pinch is determined by constructing a wire grid anode on the return current bars which are notched at 0.5 cm intervals to accurately position the anode plane. A small high voltage pin, which is located in the gas valve body, is used to create a gas discharge soon after the gas valve is opened. This distinct signature is used to time the firing of the simulator. With these geometries it has been possible to produce 50 kJ of aluminum and 20 kJ of argon K-line radiation. This has been accomplished while operating at 65% of the maximum storage capability of the marx capacitor banks.

In the next section, we will discuss the power flow limitations of the Phoenix, while in Section III we present the gas puff valve operation including its control circuitry. In Section IV, we conclude with a description of the effect of the prepulse on the plasma source.

II. Diode Power Flow

There appears to be two primary reasons that the simulator must be operated at 65% of its maximum stored energy: (1) premature insulator flashover, and (2) power flow losses in the MITL. Under ideal operation the diode insulator is designed to flashover during the positive, reflected voltage wave arising from the impedance miss-match caused by the plasma implosion. Premature flashover during the forward-going, negative primary power pulse reduces the current available to the diode load. Operation at the lower charge voltage has reduced the occurrence of early time flashover. An associated reason for operating at reduced energy has been the desire to achieve acceptable insulator lifetime by slowing the permanent damage due to "wormholing" in the polyurethane insulator rings. Both the flashover and bulk insulator damage were observed to occur at electric fields well below the generally accepted breakdown criteria. This suggested that the cause was a nonuniform field distribution across the insulator stack; attributed to either the basic insulator geometry or due to early flashing of a weak insulator ring. Detailed inspection of the damage patterns in the insulator rings suggested that the bosses (used to retain the o-ring) on the stainless steel grading rings were initiating wormholing as flashover shorted out segments of the insulator stack leading to higher stresses on the remaining sections. In turn, after their formation, the wormholes contributed to poor field grading leading to unsatisfactory flashover performance. Other potential contributing factors were identified as the exposure of the insulators to UV and soft x-rays and mechanical stresses due to slippage of the vacuum tube hardware. In order to allow higher voltage operation, a new insulator design has been completed and is currently being fabricated.

The new design reduces field stress by removing the o-ring bosses that protrude into the plastic insulator and uses a design that embeds the o-ring inside the stainless steel grading ring. This allows the insulating surface to be flat and free of field enhancements. The plastic insulator thickness was also increased by 3.8 mm (0.150") to 22.9 mm (0.900"). The design change requires the use of bosses on the periphery of the grading ring to maintain the concentricity of the insulating rings. In addition, the new design uses nine insulator rings, rather than the existing eight, which are centered with-respect-to the water flare. With this configuration the calculated field uniformity ranges from +6% to -10% about the mean. Although this insulator design increases the diode inductance somewhat, circuit analyses estimate an 18% increase in current is achievable when the simulator is operated at 85 kV charge.

Figure 4, illustrates the effect of MITL separation on the coupling of energy to an aluminum wire plasma load. The data points, which are representative of three shots for each wire diameter, were collected to determine the sensitivity of the PRS output to array and wire diameter. This data also indicates that the radiation output increases as the MITL separation is changed from 8 mm to 10 mm. This is despite the associated increase in diode inductance which lowers the available diode current. Since the radiation should be a function of the square of the diode current, the sensitivity on the MITL gap separation is relatively strong. At this time, data at wider separations have not been taken.

The explanation for this result is not yet understood. The increased MITL spacing allows increased direct-line exposure of the insulator stack and vacuum transmission line surface to ultra-violet radiation from the PRS. This suggests that the increased illumination does not contribute to poorer performance under these conditions. The small gap does increase the electric fields, which

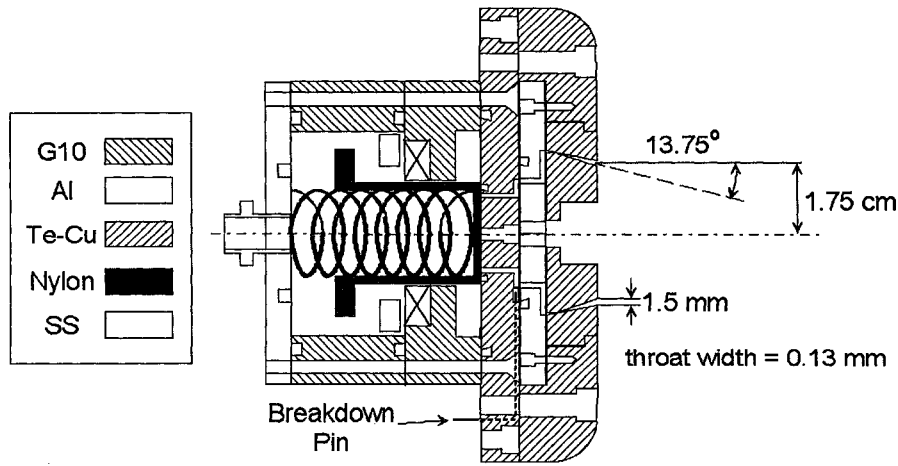


Figure 3. Schematic drawing of the Phoenix puff gas valve

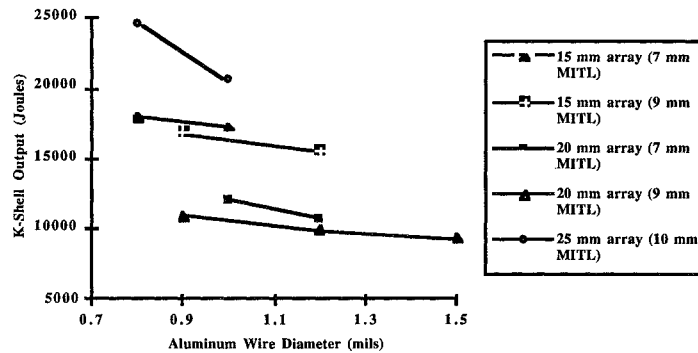


Figure 4. Effect of MITL separation on radiation source output.

may cause early time plasma formation in the MITL, leading to poorer power transfer. Alternatively, it may be that there is significant vacuum current which is intercepted by the anode structure close to the load entrance, in the region where the conical section transitions to the axial load geometry.

The rise time of the Phoenix main voltage pulse is on the order of 50 ns, which is much longer than the length of the vacuum transmission line; approximately 1.5 meters \approx 5 ns. This suggests that the diode current should be dominated by the load characteristics, with little vacuum current in the MITL gap.² Diode currents are measured with segmented Rogowski coils located at the near the vacuum insulator and with two sets of resistive monitors located in the MITL anode plate at 30 cm and 15 cm from the load. The Phoenix MITL geometry makes it difficult to measure the cathode current which would provide a direct estimate of the vacuum current.

III: Gas Valve Operation

The gas valve is located in the electric-field free region inside the cathode MITL. The lack of a transit-time isolator posed some interesting design problems for the gas valve control circuitry. Neither gas lines nor power and control cables could be passed across the large potential between the water-dielectric transmission line electrodes. Because of this restriction, several methods had to be improvised to achieve satisfactory operation: (1) batteries operating in vacuum had to be used to supply the electrical power for actuating the gas valve and the control transducers; (2) problems

with supplying sufficient heat conduction to operate in the vacuum environment had to be overcome; (3) all control circuits (e.g. pressure monitoring, triggering, electrical charging) are operated by fiber optic lines from the simulator control room; and (4) electrical vacuum break down had to be avoided.

In order to set the required gas valve plenum pressure, a technique was developed to reduce the uncertainty in obtaining the required absolute pressure with the valve hardware at full atmosphere. Figure 5 illustrates the gas valve plumbing. A small vacuum chamber was constructed to house a standard pressure regulator. With this small chamber evacuated the regulator is used to set the required absolute pressure directly. In order to operate the puff gas valve below atmospheric pressure, it has been necessary to incorporate a remotely operated valve which allows evacuating the gas line connecting it and the puff gas valve when the Phoenix diode is under vacuum.

Use of this design has provided reliable and repeatable operation. Power requirements are low enough that batteries need recharging only at the end of the day. No problems of operating the

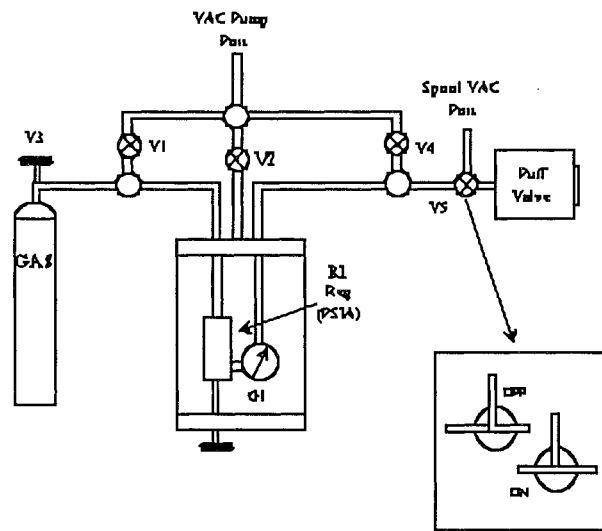


Figure 5 Illustration of gas valve control logic. Step 1: Manually open valves V1, V2, and V4 and close valve V3 and set V5 off, then evacuate regulator chamber and connecting lines. Step 2: Manually close valves V1, V2, and V4 and open valve V3 to set absolute pressure on gauge G1. Step 3: Evacuate diode and after line connecting puff gas valve to V5 is evacuated, remotely turn on V5. This three step process allows operation at absolute pressures below ambient atmosphere.

batteries in the vacuum environment have been observed.

IV: Prepulse Effects

The Phoenix pulsed power circuit has been modeled extensively using SCREAMER³ and other transmission line computer codes. One objective of these calculations has been to predict the prepulse voltage which appears at the diode due to charging of the PFL. The effect of prepulse energy is expected to be different for wire arrays and gas puff loads.

Wire arrays present an approximate short circuit to the prepulse. Peak prepulse currents on the order of 15 kA were measured in wires for about 250 nsec prior to the arrival of the main

pulse. These currents were measured using the resistive shunt monitor located about 15 cm from the cathode end of the wire load; this is the same monitor used to determine the load current during the main pulse and accuracies are within 10%. To obtain the prepulse current measurement, a power tee was placed in the signal cable and one leg was sent to a digitizer used on a sensitive scale. These measurements indicate that the energy deposited in the wires is in the range of 5-8 J. For 0.8 mil, 4 cm long aluminum wires this is sufficient to bring the wires to partial or total vaporization. The measured prepulse energy agrees well with the computer model predictions. Simple calculations indicate that very little motion of the wires should occur over the period of the prepulse voltage.

During gas puff operation, computer models indicate that an open circuit voltage (equivalent to voltage appearing across a gas load prior to break down) is expected to be on the order of 70 kV during the prepulse phase. Measurement of the gas prepulse voltage indicate that the actual levels are 40 kV or less with peak currents reaching 20 kA. This is sufficient to create a significant discharge in the low density gas. While the energy delivered to the gas puff during the prepulse phase is insignificant compared to the energy of the main pulse, the breakdown paths established through the gas may form the initial conditions which determine what portions of the gas distribution are included in the implosion. Efforts are presently underway to determine, both theoretically and experimentally, the gas current distribution at the time of arrival of the main pulse.

As part of the experimental effort, an imaging camera will be set up to view the gas plasma both end on and side on. Preliminary measurements were made with a 925 μm diameter, quartz fiber optic cable placed inside the Phoenix vacuum chamber to view the wire and gas PRS implosion side on from a position of about 25 cm away from the source. The fiber was connected to a photo multiplier tube with an S-4 response inside the facility, RF-shielded data room. The combination of fiber and photo-multiplier gave maximum sensitivity to visible light (approximately 300 nm to 600 nm). Neutral density filters were placed between the detector and the end of the fiber optic to view various illumination levels as they appeared during the formation of the PRS; no attempt was made to quantify the amplitudes of visible light for the various discharges, but timing of the fiber signal relative to electrical signals was correlated to within one nanosecond.

For wire loads, first light was observed with the arrival of the prepulse, about 250 nsec prior to the main pulse. The light level remained relatively constant throughout the prepulse. For gas loads, first light appeared with the erection of the marx about 1.5 μsec prior to diode arrival of the main pulse. This relatively low light level signal continued until the arrival of the prepulse which produced a signal level about 1000 times brighter. This prepulse light signal tracks the prepulse current monitor and has a relatively fixed intensity. The main pulse produced a recorded light signal several million times brighter than the lowest level signals recorded during the marx discharge. This bright light appears to track the main pulse current with no obvious decrease in visible light amplitude as the plasma reaches higher temperatures.

V: Acknowledgments

The authors wish to acknowledge the contributions of the Phoenix technical staff for their excellent work in operating and maintaining the equipment. They also wish to express appreciation for the support and encouragement of Mr. Leonard Pressley, Defense Nuclear Agency.

* This work was supported by the Defense Nuclear Agency under MIPR 94-529. Amendment #2.

^a Present address: Micro Craft Technology, Arnold AFB, TN 37389-6400.

^b Present address: Naval Surface Warfare Center, Dahlgren Division, Silver Spring, MD 20903-5640.

^c Supported under National Research Council Postdoctoral Program.

^d Present Address: Alameda Applied Sciences Corporation, Oakland, CA 94611-3112.

^e Present address: Garron Instrument Engineering, Eugene, OR 97405.

¹ G. G. Peterson and B. V. Weber, IEEE Conference Record-Abstracts, 1995 IEEE International Conference on Plasma Science, 5-8 June 1995, Madison Wisconsin; G. Peterson, et. al, Journal of Applied Physics, (To be submitted).

² John M. Creedon, Journal of Applied Physics, Vol 48, No. 3, March 1977, p 1070.

³ Mark L. Kiefer, Kelley L. Fugelso, and M. M Widner, SCREAMER: A Pulsed Power Design Too, Users's Guide, June 26, 1991.